Assessing the impact of resolution and soil datasets on flash-flood modelling

Alexane Lovat[1], Béatrice Vincendon[2], and Véronique Ducrocq[1]

[1]CNRM PRECIP (Météo France, CNRS), 42 av. G. Coriolis, 31057 Toulouse cedex 1, France
[2]DCSC Météo France, 42 av. G. Coriolis, 31057 Toulouse cedex 1, France

Correspondence: Alexane Lovat (alexane.lovat@meteo.fr)

Abstract. The present study assesses the impacts of two grid resolutions and the descriptors of soil texture and land cover on flash-flood modelling at local and basin scales. The ISBA-TOP coupled system, which is dedicated to Mediterranean flash-flood simulations, is used with two grid-cell sizes (300 m and 1000 m), two soil texture datasets and two land use databases, to model 12 past flash-flood events in southeastern France. The skill of the hydrological simulations is assessed using conventional data (discharge measurements from operational networks) and proxy data such as post-event surveys and high-water marks. The results show significant differences between the experiments in terms of both the simulated river discharge and the spatial runoff, whether at the catchment scale or at the local scale. The spatial resolution has the largest impact on the hydrological simulations. In this study, it is also shown that the soil texture has a larger impact on the results than the land cover.

1 Introduction

Devastating flash floods triggered by heavy precipitation events occur in the Mediterranean coastal regions primarily in autumn (Ricard et al., 2012). The mesoscale convective systems associated with these precipitating events and the geomorphologic characteristics of the region can lead to short hydrological response times ranging from a few minutes to a few hours. These floods represent a significant hazard to human safety and a threat to property and have caused at least 85 billion euros of damage since 1900 in the countries surrounding the Mediterranean Sea (Gaume et al., 2016). Accurate simulations and forecasts of the hydrologic behaviour of these catchments, such as the runoff produced during a precipitating event, are essential to identify exposed areas, issue effective warnings and guidance and notify at-risk populations. Nevertheless, the complex space–time features of Mediterranean precipitating systems make flash floods particularly difficult to model and forecast. Several hydrological models are devoted to this type of event. Such models are designed to properly simulate fast responding river discharge and the areas where runoff is produced. For floods or flash floods, the forecast ability depends not only on the spatial and temporal accuracy of the rainfall forcing (Van Steenbergen and Willems, 2014; Vivoni et al., 2007; Garambois et al., 2015) but also on the model description of the physical and hydrological characteristics of the watershed (Cotter et al., 2003; Marchi et al., 2010). Several authors have studied how to account for uncertainties associated with meteorological data, initial soil moisture and hydrological model parameters. Zappa et al. (2011) have investigated the propagation and the superposition of these three sources of uncertainty in a hydrometeorological forecasting system for a catchment of the Swiss

Alps. Meteorological data uncertainties have been addressed using high-resolution ensemble numerical weather predictions to issue probabilistic discharge forecasts (Ferraris et al., 2002; Vincendon et al., 2011; Hardy et al., 2016). Other methods have also been studied, such as the post-processing of deterministic quantitative precipitation forecasts (Vincendon et al., 2011) or the use of bias correction techniques (Zalachori et al., 2012) or multi-model numerical weather prediction (NWP) forecasts (McBride and Ebert, 2000). The coupling of meteorological ensemble prediction systems with hydrological ensemble systems has been notably studied in HEPEX (the Hydrologic Ensemble Prediction EXperiment, Schaake et al., 2007). The sensitivity of the hydrological models to the initial soil moisture (e.g. Silvestro and Rebora, 2014) and to hydrological parameters (e.g. Liu et al., 2012; Edouard et al., 2018) have also been extensively studied in the past. Based on such a sensitivity study, Edouard et al. (2018) designed an ensemble prediction system for flash-flood forecasting. In addition, hydrological modelling uncertainties arise from the soil and land descriptions. Elevation, land use and soil texture datasets are available at various spatial resolutions and from various data providers. Many hydrological models are calibrated, and the value of the calibrated parameters may depend on such terrain descriptors. Several studies have investigated the impact of soil and land data and their resolution using various digital elevation model (DEM), land cover (Kamali et al., 2017; Yen et al., 2015; Sharifi and Kalin, 2010) and soil datasets (e.g. the Soil Survey Geographic database and the State Soil Geographic database) (Kumar and Merwade, 2009; Chaplot, 2014; Cotter et al., 2003). The influence of the model resolution, which is strongly linked to the soil and land data resolution, has also been investigated (Vázquez et al., 2002; Egüen et al., 2012). Even if in general higher resolution leads to more accurate simulations, there can be a critical level beyond which the model response is not necessarily improved (Hengl, 2006; Egüen et al., 2012). Land use and in particular, preferential pathways, can have a large impact on the catchment residence times and the time flood wave travels (Blöschl, 2001; Blöschl et al., 2007). Several studies have identified the most appropriate model structure in hydrological modelling while taking into account several landscape complexity levels (e.g. Flügel, 1995; Savenije, 2010; Gharari et al., 2014b, a). Gharari et al. (2014a) have used models of increasing complexity (the first represents the catchment in a lumped way, the second distinguishes wetlands from the remainder, i.e., hillslopes and plateaus and the third gives a complete representation of the wetlands, hillslopes and plateaus). They showed that by allowing for more landscape-related process heterogeneity in a model (third model), the predictive power increases even without traditional calibration. The impact of the representation of the soil and land properties on flash-flood modelling remains poorly explored, even though these descriptors are expected to influence the timing of the flash-flood prediction and the spatial and temporal distribution of the runoff. Of the few studies dedicated to flash floods, Rozalis et al. (2010) used an uncalibrated hydrological model based on the SCS curve number method (SCS, 1964) to simulate the effect of land use changes and urban development on the flash-flood intensity over a Mediterranean watershed in Israel. Antonetti et al. (2016) explored recently the uncertainty of hydrological simulations due to different spatial representations of dominant runoff processes. They found that the simulations with the most complex automatic mapping approach are the closer to the reference map, while those without soil information differed considerably. Anquetin et al. (2010) investigated the impact of the soil spatial variability on the simulated discharge for an extreme event in southern France. Their results identified two phases in the flood dynamics: the first one was primarily controlled by the soil properties and the second one, after soil saturation, was controlled by the rainfall variability. If the soil properties are simplified in the hydrological model (catchments were described using only their major soil type), the resulting

misestimation of the maximum storage capacity of the catchment leads to large errors in the flow simulation (Anquetin et al., 2010).

The present study investigates the impacts of the spatial resolution and terrain descriptors on flash-flood modelling using the ISBA-TOP hydrological model (Bouilloud et al., 2010; Vincendon et al., 2016), which is dedicated to Mediterranean flash-flood simulations. Two grid resolutions (300 m and 1000 m) and soil datasets are used with ISBA-TOP to simulate several past flash-flood events in southeastern France. Validating a flash-flood discharge and runoff simulation is extremely challenging. Indeed, the lack of surface runoff observations is a real impediment to evaluating a runoff simulation at the proper spatial scale. The streamflow measurements, which are classically used for discharge evaluations, are only sparsely available in this region. Many of the small watersheds affected by Mediterranean flash floods are ungauged. It is therefore necessary to seek other data indirectly related to the flash-flood magnitude that can provide valuable information on various aspects of the floods, such as the spatial expansion of the flood or its duration. Such proxy data include terrain in-situ measurements, photos and water marks. In the framework of the HyMeX (Hydrological cycle in Mediterranean Experiment) project (Drobinski et al., 2014; Ducrocq et al., 2014), post-event surveys have been conducted to document the characteristics and consequences of floods, even in ungauged catchments (Payrastre et al., 2015, 2016). A very recent database gathered flood-related damage data since 2011 in the south of France at a fine scale (Saint-Martin et al., 2018). Javelle et al. (2014) demonstrated that these data provide valuable information for evaluating the simulated flood peak. New approaches are being explored to use flood-damage and runoff-impact data to evaluate the simulated runoff. For example, Vincendon et al. (2016) compared flooded area diagnoses with road-cut data and Lagadec et al. (2016) used information from post-event surveys to evaluate a method to map the susceptibility to surface runoff from the impact of floods on a railway.

To investigate and rank the impacts of the spatial resolution and the terrain descriptors on flash-flood modelling, two spatial scales (catchment and local scales) are studied using conventional data as well as proxy data to assess the ISBA-TOP simulations, i.e. discharges measurements, post-event surveys and high-water marks are used to evaluate the hydrological model outputs. This paper is organized as follows. Section 2 describes the study region, the hydrological system used and its input datasets. The runoff model sensitivity to the grid resolution and the soil descriptors at different scales over several catchments is examined and discussed in Section 3. The conclusions are given in Section 4.

2 Materials and methods

2.1 Case study

The catchments of interest are located in southern France (Figure 1). Two areas representative of rural and urban land use were chosen to investigate the impact of the soil properties on the performance of the hydrological model. The topography of both areas varies greatly from the sea level up to 1750 m with steep slopes and narrow valleys. The catchments have short response times, with rivers responding to rainfall events within approximately 2–7 h (see Table 1).

The rural zone 'A' consists of four catchments in the Cévennes region: the Lergue River at Lodève (181 km^2), the Hérault River at Laroque (918 km^2), the Gardon River at Ners (1092 km^2) and the Vidourle River at Sommières (621 km^2) (Ta-

ble 1). For the larger catchments, the simulations are also compared at the outlets of their sub-catchments. The Cévennes watersheds are prone to flash flooding, and their rivers are well monitored by the French flood forecasting service (SCHAPI). The Cévennes-Vivarais catchments have long been observed by the Cévennes-Vivarais Hydro-Meteorological Observatory (OHM-CV, Boudevillain et al., 2011). In addition, the FloodScale project (a multi-scale observation and modelling strategy for understanding and simulating flash floods, Braud et al., 2014), which contributes to the HyMeX international program, performed enhanced observations for four years (2012–2015) in this region. A total of 11 recent flash-flood events occurring in zone A between 2014 and 2016 were considered in this study (Table 2). These were single or two-flow peak events and are representative of the variety of rainfall intensities and durations and the hydrological responses of the rivers encountered in the Cévennes-Vivarais region.

(Fig 1 around here)

The French Riviera was selected as the urban domain (Figure 1) because it was affected by the last catastrophic flash-flood event in southern France on 03 October 2015 in the Cannes area. The urban zone 'B' consists of four main catchments and two coastal areas. The catchments are the Siagne River at Pégomas (515 km^2), the Loup River at Villeneuve-Loubet (278 km^2), the Cagne River at Cagnes-sur-mer (109 km^2) and the Brague River at Biot (41 km^2) (see Table 1). Only a few watersheds are monitored in this region and some basins are ungauged. In this study, eight discharge outlets were used; of these, three are monitored by SCHAPI. In the following, the outlets will be called O# if they are operationally gauged by SCHAPI and E# if their peak discharge values or water levels are estimated from post-event surveys or proxy data.

(Table 1 around here)

(Table 2 around here)

2.2 The hydrological model ISBA-TOP

The distributed hydrological model ISBA-TOP (Bouilloud et al., 2010; Vincendon et al., 2016) was designed to predict flash floods in small to medium sized Mediterranean basins. The ISBA-TOP system is a coupling between the land surface model ISBA (Interaction Surface Biosphere Atmosphere, Noilhan and Planton, 1989) and TOPODYN (Pellarin et al., 2002). ISBA manages the soil water and energy budgets between the soil vegetation snow column and the atmosphere above natural land surfaces. TOPODYN is a variant of the hydrological model TOPMODEL (Beven and Kirkby, 1979) dedicated to flash-flood modelling in Mediterranean regions. It deals with the lateral redistribution of the soil moisture according to the topographical information and the spatial variability of the rainfall.

First, ISBA computes the water and energy fluxes within the soil column for all the grid meshes in its domain. From the resulting volumetric water content, the water-storage deficit is computed by TOPODYN for each watershed pixel with a

resolution of 50 m × 50 m. The lateral distribution of the water along the watershed follows the principles of TOPMODEL using topographical indexes. The new deficits and new soil moisture fields provide ISBA with new water contents. The pixels with a null deficit indicate the saturated contributing areas. From these areas, ISBA computes the sub-surface runoff and deep drainage, which are routed to the river. The total discharges are then produced at the watershed outlets.

As part of the international HyMeX program, the ISBA-TOP coupled system has been used for real-time prediction of discharge for four catchments in the Cévennes-Vivarais region and the French Riviera, during the first Special Observation Period of Hymex, from 05 September to 06 November 2012. Case studies have also been performed with ISBA-TOP for Italian (Nuissier et al., 2016) watersheds. ISBA-TOP is also currently used in real time by the National Institute of Meteorology and Hydrology (NIMH) of Bulgaria for operational flood forecasting for the Arda River Basin (Artinyan et al., 2016).

2.3 Soil characteristics

2.3.1 Soil texture

The sensitivity to the soil texture (the proportion of clay, sand and silt) in ISBA-TOP was assessed using two different datasets: the Harmonized World Soil Database (HWSD, version 1.2, Nachtergaele et al., 2012) and the Land Use and Cover Area frame Statistical survey (LUCAS) topsoil data (Ballabio et al., 2016).

HWSD has global coverage at a resolution of 30 arcseconds (corresponding to approximately 1 km at the equator). It combines soil information from several sources worldwide, including from the European Soil Database, various regional SOTER databases (SOTWIS Database) and the Soil Map of the World database (http://www.iiasa.ac.at/Research/LUC/External-World-soil-database/HTML/). Tubiello et al. (2016) estimated the accuracy of the HWSD soil information to be approximately 75%. The LUCAS dataset covers the European Union (EU) countries at a resolution of 500 m. The soil properties were produced from the soil characteristics of the European Soil Database combined with the HWSD data. Ballabio et al. (2016) provided a map of the standard deviation (see their Figure 7), which shows that, for zones A and B, the uncertainty is low, except for areas above 1000 m (corresponding to the upper part of the Siagne, Cagne and Loup rivers in zone B), where the errors are large.

Figure 2 shows the clay and sand contents over southeastern France from HWSD and LUCAS, respectively. The mean soil texture fractions per watershed are reported in Table 3. In HWSD, the soil is mostly clay for the Vidourle and the southern part of the Hérault catchments (33–38%), whereas sand is dominant for the Gardon and Lergue catchments (approximately 40%). The spatial distribution of the soil texture is not so highly contrasted for LUCAS. In this second dataset, there is less clay over the Vidourle and Hérault catchments. For zone B, the proportions of sand in HWSD are little higher than those of clay (38% versus 24%, respectively). For the southwestern part of zone B, the proportion of clay is particularly low. LUCAS generally reports less sand than HWSD for zone B.

Soil texture has an impact on simulated runoff through soil hydrodynamic parameters, which are determined by CH78 pedotransfer functions (Clapp and Hornberger, 1978) in ISBA-TOP. Edouard et al. (2018) investigated the impact of these parameters on runoff simulations.

(Fig 2 around here)

2.3.2 Land cover

The land cover type (e.g. forest, grass, crop, rock, town or sea) of each ISBA grid mesh is initialized with the ECOCLIMAP II (Masson et al., 2003; Faroux et al., 2013) land ecosystem database at a resolution of 1 km. Over Europe and the Mediterranean basin, ECOCLIMAP includes 273 landscape types, resulting from the merging of satellite data, i.e. the Corine Land Cover 2000 product over EU countries at a resolution of 100 m, the Global Land Cover 2000 global database and the SPOT/VEGETATION satellite data. In ISBA-TOP, the urban cover of ECOCLIMAP II is considered to be a rocky cover to simulate the impervious surfaces of towns.

ECOCLIMAP Second Generation (ECOCLIMAP-SG, https://opensource.umr-cnrm.fr/projects/ecoclimap-sg/wiki/Wiki) is the latest version of ECOCLIMAP and is currently developed at a resolution of 300 m. It is based on the ESA CCI Land Cover product at a resolution of 300 m (version 1.6.1, 2016, epoch 2010 from 2008 to 2012), which gathered satellite MERIS and SPOT-VGT data. To adapt the ESA CCI covers to the land cover types of ECOCLIMAP-SG, other data sources were compiled, such as the SRTM Water Body Data from the USGS, the Global Land Cover 2000 and the Corine Land Cover 2012. In this paper, the urban grid points of ECOCLIMAP-SG are considered to be either a fraction of bare soil, bare rock, temperate broadleaf deciduous and swamp areas (called ECO-SG) or bare rock (called ECO-SG-TownToRock).

In Table 3, the mean fractions of the land use types from ECOCLIMAP and ECO-SG are given. In ECOCLIMAP, a high percentage of every watershed in zone A is covered by forests (40–56%) and grass (28–34%). In general, ECO-SG presents even more forests (40–75%) and less urban/bare soils in this area. For zone B, the land use has a higher degree of contrast between the watersheds. In ECOCLIMAP, the soil is primarily covered by forests in the largest catchments of Siagne and Loup (37–48%), whereas urban areas and towns are dominant in the Cagne and Brague catchments (approximately 40%). For this zone, ECO-SG presents less forested areas than ECOCLIMAP but more crops. The proportions of urban/bare soils are of the same order for both datasets.

In ISBA-TOP, the land cover product influences both interception storage (through the leaf area index, vegetation height and roughness length) and infiltration capacity (through the root depth), with resulting impacts on the simulated surface runoff amounts.

(Table 3 around here)

2.4 Experiments

Several experiments (see Table 4) were designed to assess the sensitivity of the simulated hydrological response to the horizontal resolution (R), the soil texture (T) and the land cover (C). ISBA was run with two different regular grids at resolutions of 300 m and 1000 m to assess the impact of the horizontal resolution. These two resolutions were selected, because the spatial

resolution of meteorological forcing data used in this study is 1km and because the new land ecosystem database ECOCLIMAP Second Generation is produced at a 300m resolution. The ISBA grid orography for each grid resolution was averaged from the Shuttle Radar Topographic Mission (SRTM) 90-m digital elevation data (Figure 1), which have a vertical accuracy of +/-16 m at the 90% confidence level (Jarvis et al., 2004). Note that the watersheds in TOPODYN are described by a Digital Terrain Model with a horizontal resolution of 50 m regardless of the ISBA grid resolution. The soil texture (from HWSD or LUCAS) and land cover (from ECOCLIMAP II or ECOCLIMAP-SG) were interpolated onto the ISBA grid. ISBA-TOP was run using five combinations of the available soil datasets. The first experiment, called ($R_1T_1C_1$), corresponds to the conventional use of ISBA-TOP (e.g. Vincendon et al., 2016) at a resolution of 1000 m with HWSD and ECOCLIMAP II. The second experiment (called $R_2T_1C_1$), changed the resolution from 1000 m (R_1) to 300 m (R_2) to investigate the impact of the resolution. Three other experiments were performed at a resolution of 300 m. The $R_2T_2C_1$ experiment evaluated the sensitivity to the soil texture by replacing HWSD (T_1) with the LUCAS topsoil (T_2). Then, the sensitivity to the land cover was evaluated by replacing ECOCLIMAP II with ECO-SG in the $R_2T_2C_2$ experiment. The last experiment, called $R_2T_2C_3$, tested the impact of the representation of the urban areas by replacing ECO-SG with ECO-SG-TownToRock.

For all the experiments, ISBA-TOP was driven by the hourly 1-km^2 quantitative precipitation estimates (QPE) ANTILOPE, which merged observations from the Météo-France radar and the rain gauges network (Laurantin, 2008). The initial conditions (soil water and soil temperature) come from the Météo-France operational hydrometeorological system SAFRAN-ISBA-MODCOU (SIM, Habets et al., 2008), which provides the hourly soil water index (SWI) and soil temperature at a resolution of 8 km over France. The data were downscaled over the 1-km ISBA domain, using the nearest-grid-point interpolation method as in (Edouard et al., 2018).

(Table 4 around here)

3 Results

3.1 Analysis at the catchment scale

3.1.1 River discharges in zone A

To compare the different experiments, several skill scores (described in Appendix B) were used. The Nash–Sutcliffe efficiency (NSE, Nash and Sutcliffe, 1970) was computed considering the catchments and sub-catchments together and separately for all the events in zone A (Figure 3) to assess the overall simulated hydrograph. Streamflow measurements were provided by the French HYDRO databank (http://www.hydro.eaufrance.fr/). The uncertainty in the discharge measurement in this databank is approximately +/-10%. In Figure 3, the closer the points are to the bottom-right corner, the better the skill. The experiment $R_2T_2C_1$ has the best score, followed by $R_2T_1C_1$. The $R_1T_1C_1$ experiment generally performs worse than the others.

(Fig 3 around here)

Figure 4a displays the LNP cost function (Roux et al., 2011). Compared to the Nash cost function, the LNP cost function grants more importance to the peak flow value and the timing. It consists of a linear combination of the Nash criterion and the error of the peak time and discharge (as defined by Lee and Singh, 1998). The differences between the simulated and observed peak values and times are also displayed in Figure 4. As for NSE, these scores were computed over the entire data sample available for zone A using the 11 cases for all the outlets and monitored sub-watersheds taken separately and together. The accuracy of the discharges simulated with the different configurations depends on the catchments; however, some general tendencies can be extracted. The scores obtained for $R_2T_1C_1$ at a resolution of 300 m are generally better than those obtained for $R_1T_1C_1$ at a resolution of 1000 m. The increase in the grid resolution appears to significantly improve the simulated peak time (see Figure 4c). This might be due to the more detailed description of the river network and of the average slope over the watershed which influence the flow velocity (Dutta and Nakayama, 2009; Vázquez et al., 2002). The timing of the simulated peak is even better with the other experiments ($R_2T_2C_1$–$R_2T_2C_3$). $R_2T_2C_2$ and $R_2T_2C_3$ give very similar results for every score of Figure 3 and Figure 4. In general, the best measures of the goodness-of-fit are obtained with $R_2T_2C_1$. The differences in the soil texture databases, which impact the water storage capacity and the ease of water to move through saturated soil, resulted in the most visible and beneficial changes in the simulated discharges. It was expected that fine-resolution input data (LUCAS, ECO-SG) would provide a better model performance for the hydrological simulations than coarser ones (HWSD and ECOCLIMAP); however, depending on the watershed (O1, O10 and O11), the opposite can be seen in Figure 4b. The scores show that the hydrological response is less sensitive to the land use data (compare $R_2T_2C_1$ and $R_2T_2C_2$) than to the soil texture data (compare $R_2T_1C_1$ and $R_2T_2C_1$); however, this result could be biased by the nearly homogeneous soils present in zone A (a large amount of forests and only a few cities, Table 3).

(Fig 4 around here)

3.1.2 Runoff over zone A

To study the impact of the resolution, land use and soil texture on the simulated runoff and to compare the simulations to each other, the runoff values computed at each ISBA-TOP grid point were cumulated over the entire event and divided by the associated amount of surface rain at the corresponding grid point during the event to take into account the spatial variability of the precipitation of each event. The differences in these ratios (the runoff amounts over the rainfall amounts) between $R_2T_1C_1$ and $R_2T_2C_1$, between $R_2T_2C_1$ and $R_2T_2C_2$ and between $R_2T_2C_2$ and $R_2T_2C_3$, respectively, were averaged over all the events (Figure 5). The same processing was applied to compare $R_1T_1C_1$ with a resolution of 1000 m to $R_2T_1C_1$ with a resolution of 300 m after resampling at the same resolution using a nearest neighbour interpolation. Enhancing the resolution results in an increase in the runoff production nearly everywhere (Figure 5a). The few red–orange or dark green isolated spots (e.g. in the southeast of O6) may be explained by the large local height differences between the higher resolution model orography at 300

m and the smoother orography at 1000 m. The change in the soil texture map (Figure 5b) leads to high disparities in the spatial patterns of the surface runoff within the study domain. In general, $R_2T_1C_1$ produces more runoff than $R_2T_2C_1$, especially over the three more southerly watersheds where the clay fraction is higher with HWSD (see O1, O5 and O11 in Table 3). This excess runoff is consistent with lower infiltration and drainage capacity associated with clay-rich soils. The areas with negative differences (green areas) often match areas with a minimum of clay in the HWSD database (see Figure 2). The change in land use (Figure 5c) leads to the largest discrepancy between the different experiments at a resolution of 300 m. Indeed, the mean differences in the ratios between the runoff and the rainfall range from -1.2 to 0.7 for $R_2T_2C_1$-$R_2T_2C_2$, whereas for $R_2T_1C_1$-$R_2T_2C_1$, that is, when changing the texture, the range of the variation is between -0.4 and 0.3. The simulations based on the land cover obtained from ECOCLIMAP-II show higher runoff amounts than ECO-SG (Figure 5c), except south of the urbanized axis, O6–O8, where the difference is high. These amounts of surface runoff produced with $R_2T_2C_2$ in this catchment appear to be correlated to the amount of settlement areas and impervious areas in the catchment. The differences between $R_2T_2C_2$ and $R_2T_2C_3$ are less pronounced than those between $R_2T_2C_1$ and $R_2T_2C_2$, except on the east side of the O8–O9 axis and next to O1, O5 and O6, where the pixels are more greenish than the surrounding pixels.

(Fig 5 around here)

3.1.3 Urbanized catchments of zone B

To confirm the results obtained for zone A, the impact of various grid resolutions and soil datasets on simulations of the discharge and runoff were assessed for the more urbanized catchments of zone B. The percentages of urban cover and impervious soils in the catchments of zone B range from 16% to 54% (Table 3). The impacts were assessed for the catastrophic October 2015 event, which affected these watersheds. Extreme downpours and flash floods wreaked havoc over the French Riviera during this event. More than 270 mm of rain fell in the most affected area (Figure 6).

(Fig 6 around here)

For zone B, only the upward watersheds of Pégomas, Villeneuve-Loubet and Biot are gauged. For the coastal area where the more severe precipitation occurred, the evaluation relies on estimated peak discharges from several post-event surveys conducted in the framework of the HyMeX project (Payrastre et al., 2016) and streamflow measurements from the French HYDRO database. The observed or estimated peak discharge for each watershed is displayed in Figure 7 together with the peak discharge simulated by all five experiments. ISBA-TOP simulated flood peaks of the correct order of magnitude, except for the discharge point E17. The timing of the peak was also well simulated according to Figure 8. As in zone A, for most of the outlets, increasing the grid resolution of ISBA lead to peak values closer to the observations. However, contrary to zone A, the discharge peak values simulated by $R_2T_2C_2$ and $R_2T_2C_3$ were significantly different for several watersheds in zone B. Therefore, for these watersheds, replacing the mixture of bare soil, bare rock and temperate broadleaf deciduous and swamp

areas with only rock over the urban land use type patches had an impact.

(Fig 7 and 8 around here)

The cumulated runoff for each experiment is displayed in Figure 9. The spatial patterns of the surface runoff simulated by the different experiments are consistent with the surface accumulated rainfall (Figure 6 compared to Figure 9). Differences between the experiments appear primarily east and north of O15, as well as at the limit between the two coastal zones, west of E18. The areas of simulated high runoff match the observed impacts zones (Figure 10), which are located near the coast and close to O15.

(Fig 9 and 10 around here)

The matching of the impacts and high runoff zones is assessed using a neighbouring approach, for which a circular region, centered on each 300 m grid point, slides across all the domain of Figure 9 counting the impacts of each category (victims, damage, high water marks) inside the circular region and the average runoff over the circular region. The radius of the circular area is set to 1 km, allowing to compare all the results at the coarser resolution of $R_1T_1C_1$ (i.e. 1 km) without having too much sea grid-points in the circular regions with impacts along the coast. Figure 11 shows the average runoff in function of the damage number. Clearly, the runoff is larger when impacts are recorded in the 1km neighbourhood, in agreement with the visual comparison between Figure 9 and Figure 10. The average runoff increases with the impact number up to 10 damages in the 1km neighbourhood. $R_2T_2C_3$ (in yellow) produces on average more runoff than the other experiments. Figure 9 shows that significant runoff is produced over a larger area for $R_2T_2C_3$. In particular, over the urbanized areas south of the upward catchments, $R_2T_2C_3$ produces more runoff than the other experiments. The largest differences between the experiments are for the 16-25 damages per circular area (Figure 11). In this range, the 1 km resolution simulation ($R_1T_1C_1$ in black) provides the lowest average value. The 16-25 damages per circular region category is mainly recorded next to O15 where $R_1T_1C_1$ produces less runoff (pink color pixels in Figure 9a).

(Fig 11 around here)

3.2 Analysis at the local scale

A detailed analysis at the local scale was performed and is illustrated here for the 12 September 2015 event affected zone A. This event was remarkable in terms of its rainfall intensity (more than 220 mm in three hours locally northeast of Lodève, called the O1 outlet) and river overflow in the Lergue Basin, that is, the smallest catchment located southwest of zone A. Four grid points (called P1, P2, P3 and P4 in Figure 12) in the city of Lodève were used to investigate differences between the experiments. At these points, the high-water levels were measured and archived on the collaborative web platform

www.reperesdecrues.developpement-durable.gouv.fr (Piotte et al., 2016).

(Fig 12 around here)

Figure 13 shows the cumulated runoff values between 3 UTC on 12 September 2015 and 8 UTC on 13 September 2015 simulated by the experiments $R_1T_1C_1$–$R_2T_2C_3$ over the red square in Figure 12. The spatial patterns of the surface runoff differ from one configuration to another and specifically with the change in the resolution (Figure 13a and Figure 13b). The distribution of runoff is obviously coarser in $R_1T_1C_1$, and the four points are in the same grid cell at a resolution of 1000 m. The change in the land cover maps also has a significant influence (Figure 13c and Figure 13d). The higher value of the runoff is located near P2 for $R_2T_1C_1$ and $R_2T_2C_1$, whereas the runoff extends south of the Lergue watershed for $R_2T_2C_2$ and $R_2T_2C_3$. The runoff is more intense for $R_2T_2C_2$ and $R_2T_2C_3$ than for $R_2T_1C_1$ and $R_2T_2C_1$, especially for points P1, P3 and P4 (see Figure 13). The runoff time series shown in Figure 14 leads to the same conclusion. The higher peak values for experiments $R_2T_2C_2$ and $R_2T_2C_3$ are also consistent with the measured high-water marks (Table 5) for the four points. ECO-SG and ECO-SG-TownToRock allow the observed runoff to be better represented locally. This might be due to the fact that, at P1 and P4, the land cover is primarily forest with ECOCLIMAP-II whereas ECO-SG describes these points as open midrise, involving more impervious soils.

(Fig 13 and 14 around here)

(Table 6 around here)

For the same event and next to these points, the post-event flood peaks were estimated during the intensive post-event campaigns for HyMeX. These estimations concern the Breze River at Saint-Étienne-de-Gourgas (P5), the Lergue River at Poujols (P6) and the Soulondre River at Lodève (P7). Their locations can be seen in the black square in Figure 12. The estimated and simulated peak flows are shown in Figure 15. $R_2T_2C_2$ and $R_2T_2C_3$ simulate more realistic values than $R_1T_1C_1$, $R_2T_1C_1$ and $R_2T_2C_1$ at P5 and P6 even though the values are overestimated.

(Fig 15 around here)

4 Conclusions

The representation of the soil and land properties in hydrological models is crucial for flash-flood simulations in addition to other data concerning the rainfall and the initial state of the soil moisture. The impact of these terrain descriptors on predictions in terms of both the spatial and temporal distributions of the runoff has not been fully explored.

In this study, different sources of soil texture and land use data were used to describe two areas (a rural area and an urbanized area) in southeastern France using the ISBA-TOP system run at two different resolutions (300 m and 1000 m). The model performances, especially in terms of the runoff simulations, are difficult to assess. The results were analysed to rank the impacts of alternative physiographic maps for flash-flood modelling purposes at the catchment scale and at the local level. Discharge measurements, as well as proxy data such as post-event surveys and high-water marks, were used depending on their availability.

The main conclusions from this study are as follows.

- Changing the resolution of ISBA-TOP leads to differences in terms of the simulated river discharge and the spatial runoff. Higher resolution, 300 m, simulations give more accurate results.

- The simulated discharge values are often more affected by differences in the soil texture databases than differences in the land use databases, especially in rural areas.

- No significant difference in the peak time was found when comparing the different 300-m experiments.

- Land cover and soil texture influence locally the processes in the catchments. Their spatial variability has an impact on the preferential flow paths, the flow velocities and the water storage. The complexity of the interactions between processes at the catchment scale does not allow us to clearly conclude on how land cover and soil texture, induce differences in simulated flows.

- Finally, in this study, the best results were obtained using SRTM data for orography, LUCAS data for soil texture and ECOCLIMAP-II for land cover at a resolution of 300 m (i.e. the $R_2T_2C_1$ experiment).

These conclusions need to be considered with caution because the sample of events and catchments was limited, especially for the urbanized area. Moreover, it would be interesting to compare these results with those that can be obtained using other hydrological models dedicated to flash-flood modelling. For example, the higher sensitivity to soil texture than to land cover might depend on how the vegetation is treated in the model. Note that, for calibrated models, this impact might be 'corrected' during the calibration procedure. Therefore, for a different dataset, the calibrated model needs to be recalibrated. In any case, for the future development of flash-flood modelling and forecasting, the impact of soil datasets should be taken into account in the uncertainty quantification, even though this impact is less significant than those associated with the rainfall and initial soil moisture. The lack of information with regard to flash floods in ungauged catchments may constitute a real barrier to the evaluation of the simulated hydrologic responses. Fortunately, data such as impact data from post-event surveys, 'connected' measurements and georeferenced data from social networks might be useful to enlarge the capacity of the model output assessments especially during extreme events.

Appendix A: Basin characteristic times

The basin concentration time is estimated using the formulation of Bransby Williams (Almeida et al., 2015), which depends on the main channel length L, the catchment area A and the average catchment slope S: $t_c = 0.605 \frac{L}{A^{0.1} S^{0.2}}$. The basin concentration time represents the time required for a single raindrop to travel from the hydraulically most distant point in the

watershed to the outlet. The basin lag time is calculated using the formulation of the Soil Conservation Service (Maidment et al., 1993), which considers the ratio between the concentration time and lag time to be approximately 0.6. The lag time is the delay between the peak of the rain and the peak of the runoff.

Appendix B: Scores

B1 NSE

The Nash–Sutcliffe efficiency (NSE, Nash and Sutcliffe, 1970) is a normalized statistic that indicates if the simulated hydrological time series fits the observed one. Considering N simulations hours, Q_i^s is the value of the simulated hourly discharge at time i, Q_i^o is the corresponding observation and $\bar{Q^o}$ is the time-averaged observed discharge for the entire simulation. The NSE criterion tends to over-represent large flows relative to other measurements due to the squared deviations. $NSE = 1 - \frac{\sum_{i=1}^{N}(Q_i^s - Q_i^o)^2}{\sum_{i=1}^{N}(Q_i^o - \bar{Q^o})^2}$

B2 LNP

In the LNP cost function (Roux et al., 2011), N is the number of simulation hours, Q_p^s and Q_p^o are the simulated and observed peak discharges, respectively, T_p^s and T_p^o are the simulated and observed times to peak, respectively, and T_c^o is the concentration time of the catchment (see Section 2.1). $LNP = \frac{1}{3}NSE + \frac{1}{3}(1 - \frac{|Q_p^s - Q_p^o|}{Q_p^o}) + \frac{1}{3}(1 - \frac{|T_p^s - T_p^o|}{T_c^o})$

Acknowledgements. This research was performed in the framework of the HyMeX programme and is a contribution to the French project PICS. The authors would like to express their gratitude for access to useful data and discussions about ECOCLIMAP with Stéphanie Faroux within the surface department of CNRM in Toulouse. The Shuttle Radar Topographic Mission (SRTM) 90-m digital elevation data were originally produced by NASA and provided by the Consortium for Spatial Information of the Consultative Group for International Agricultural Research (CGIAR-CSI) GeoPortal (http://srtm.csi.cgiar.org/). The Harmonized World Soil Database (HWSD, version 1.2) was provided by the Food and Agriculture Organization of the United Nations (FAO) and the International Institute for Applied Systems Analysis (IIASA).

References

Almeida, I., Kaufmann Almeida, A., Ayach Anache, J., Steffen, J., and Alves Sobrinho, T.: Estimation on Time of Concentration of Overland Flow in Watersheds: A Review, 33, 661–671, 2015.

Anquetin, S., Braud, I., Vannier, O., Viallet, P., Boudevillain, B., Creutin, J.-D., and Manus, C.: Sensitivity of the hydrological response to the variability of rainfall fields and soils for the Gard 2002 flash-flood event, Journal of hydrology, 394, 134–147, 2010.

Antonetti, M., Buss, R., Scherrer, S., Margreth, M., and Zappa, M.: Mapping dominant runoff processes: an evaluation of different approaches using similarity measures and synthetic runoff simulations, Hydrology and Earth System Sciences, 20, 2929–2945, 2016.

Artinyan, E., Vincendon, B., Kroumova, K., Nedkov, N., Tsarev, P., Balabanova, S., and Koshinchanov, G.: Flood forecasting and alert system for Arda River basin, Journal of Hydrology, 541, 457–470, 2016.

Ballabio, C., Panagos, P., and Monatanarella, L.: Mapping topsoil physical properties at European scale using the LUCAS database, Geoderma, 261, 110–123, 2016.

Beven, K. and Kirkby, M. J.: A physically based, variable contributing area model of basin hydrology/Un modèle à base physique de zone d'appel variable de l'hydrologie du bassin versant, Hydrological Sciences Journal, 24, 43–69, 1979.

Blöschl, G.: Scaling in hydrology, Hydrological Processes, 15, 709–711, 2001.

Blöschl, G., Ardoin-Bardin, S., Bonell, M., Dorninger, M., Goodrich, D., Gutknecht, D., Matamoros, D., Merz, B., Shand, P., and Szolgay, J.: At what scales do climate variability and land cover change impact on flooding and low flows?, Hydrological Processes: An International Journal, 21, 1241–1247, 2007.

Boudevillain, B., Delrieu, G., Galabertier, B., Bonnifait, L., Bouilloud, L., Kirstetter, P.-E., and Mosini, M.-L.: The Cévennes-Vivarais Mediterranean Hydrometeorological Observatory database, Water Resources Research, 47, 2011.

Bouilloud, L., Chancibault, K., Vincendon, B., Ducrocq, V., Habets, F., Saulnier, G.-M., Anquetin, S., Martin, E., and Noilhan, J.: Coupling the ISBA land surface model and the TOPMODEL hydrological model for Mediterranean flash-flood forecasting: description, calibration, and validation, Journal of Hydrometeorology, 11, 315–333, 2010.

Braud, I., Ayral, P., Bouvier, C., Branger, F., Delrieu, G., Le Coz, J., Nord, G., Vandervaere, J., Anquetin, S., Adamovic, M., et al.: Multi-scale hydrometeorological observation and modelling for flash-flood understanding, Hydrology and Earth System Sciences, 18, 3733–3761, 2014.

Chaplot, V.: Impact of spatial input data resolution on hydrological and erosion modeling: Recommendations from a global assessment, Physics and Chemistry of the Earth, Parts A/B/C, 67, 23–35, 2014.

Clapp, R. B. and Hornberger, G. M.: Empirical equations for some soil hydraulic properties, Water resources research, 14, 601–604, 1978.

Cotter, A. S., Chaubey, I., Costello, T. A., Soerens, T. S., and Nelson, M. A.: Water quality model output uncertainty as affected by spatial resolution of input data, JAWRA Journal of the American Water Resources Association, 39, 977–986, 2003.

Drobinski, P., Ducrocq, V., Alpert, P., Anagnostou, E., Béranger, K., Borga, M., Braud, I., Chanzy, A., Davolio, S., Delrieu, G., et al.: HyMeX: A 10-year multidisciplinary program on the Mediterranean water cycle, Bulletin of the American Meteorological Society, 95, 1063–1082, 2014.

Ducrocq, V., Braud, I., Davolio, S., Ferretti, R., Flamant, C., Jansa, A., Kalthoff, N., Richard, E., Taupier-Letage, I., Ayral, P.-A., et al.: HyMeX-SOP1: The field campaign dedicated to heavy precipitation and flash flooding in the northwestern Mediterranean, Bulletin of the American Meteorological Society, 95, 1083–1100, 2014.

Dutta, D. and Nakayama, K.: Effects of spatial grid resolution on river flow and surface inundation simulation by physically based distributed modelling approach, Hydrological Processes: An International Journal, 23, 534–545, 2009.

Edouard, S., Vincendon, B., and Ducrocq, V.: Ensemble-based flash-flood modelling: Taking into account hydrodynamic parameters and initial soil moisture uncertainties, Journal of Hydrology, 560, 480–494, 2018.

Egüen, M., Aguilar, C., Herrero, J., Millares, A., and Polo, M.: On the influence of cell size in physically-based distributed hydrological modelling to assess extreme values in water resource planning, Natural Hazards and Earth System Sciences, 12, 1573, 2012.

Faroux, S., Kaptué Tchuenté, A., Roujean, J.-L., Masson, V., Martin, E., and Moigne, P. L.: ECOCLIMAP-II/Europe: a twofold database of ecosystems and surface parameters at 1 km resolution based on satellite information for use in land surface, meteorological and climate models, Geoscientific Model Development, 6, 563–582, 2013.

Ferraris, L., Rudari, R., and Siccardi, F.: The uncertainty in the prediction of flash floods in the northern Mediterranean environment, Journal of hydrometeorology, 3, 714–727, 2002.

Flügel, W.-A.: Delineating hydrological response units by geographical information system analyses for regional hydrological modelling using PRMS/MMS in the drainage basin of the River Bröl, Germany, Hydrological Processes, 9, 423–436, 1995.

Garambois, P.-A., Roux, H., Larnier, K., Labat, D., and Dartus, D.: Parameter regionalization for a process-oriented distributed model dedicated to flash floods, Journal of Hydrology, 525, 383–399, 2015.

Gaume, E., Borga, M., Llassat, M. C., Maouche, S., Lang, M., and Diakakis, M.: Mediterranean extreme floods and flash floods, 2016.

Gharari, S., Hrachowitz, M., Fenicia, F., Gao, H., and Savenije, H.: Using expert knowledge to increase realism in environmental system models can dramatically reduce the need for calibration, Hydrology and Earth System Sciences, 18, 4839–4859, 2014a.

Gharari, S., Shafiei, M., Hrachowitz, M., Kumar, R., Fenicia, F., Gupta, H., and Savenije, H.: A constraint-based search algorithm for parameter identification of environmental models, Hydrology and Earth System Sciences, 18, 4861–4870, 2014b.

Habets, F., Boone, A., Champeaux, J.-L., Etchevers, P., Franchisteguy, L., Leblois, E., Ledoux, E., Le Moigne, P., Martin, E., Morel, S., et al.: The SAFRAN-ISBA-MODCOU hydrometeorological model applied over France, Journal of Geophysical Research: Atmospheres, 113, 2008.

Hardy, J., Gourley, J. J., Kirstetter, P.-E., Hong, Y., Kong, F., and Flamig, Z. L.: A method for probabilistic flash flood forecasting, Journal of Hydrology, 541, 480–494, 2016.

Hengl, T.: Finding the right pixel size, Computers & geosciences, 32, 1283–1298, 2006.

Jarvis, A., Rubiano, J. E., Nelson, A., Farrow, A., and Mulligan, M.: Practical use of SRTM data in the tropics: Comparisons with digital elevation models generated cartographic data, 2004.

Javelle, P., Demargne, J., Defrance, D., Pansu, J., and Arnaud, P.: Evaluating flash-flood warnings at ungauged locations using post-event surveys: a case study with the AIGA warning system, Hydrological sciences journal, 59, 1390–1402, 2014.

Kamali, B., Abbaspour, K. C., and Yang, H.: Assessing the Uncertainty of Multiple Input Datasets in the Prediction of Water Resource Components, Water, 9, 709, 2017.

Kumar, S. and Merwade, V.: Impact of watershed subdivision and soil data resolution on SWAT model calibration and parameter uncertainty, JAWRA Journal of the American Water Resources Association, 45, 1179–1196, 2009.

Lagadec, L.-R., Breil, P., Chazelle, B., Braud, I., and Moulin, L.: Use of post-event surveys of impacts on railways for the evaluation of the IRIP method for surface runoff mapping, in: E3S Web of Conferences, vol. 7, p. 10005, EDP Sciences, 2016.

Laurantin, O.: ANTILOPE: Hourly rainfall analysis merging radar and rain gauge data, in: Proceedings of the International Symposium on Weather Radar and Hydrology, Grenoble, pp. 2–8, France, 10–12 March 2008, 2008.

Lee, Y. and Singh, V.: Application of the Kalman filter to the Nash model, Hydrological Processes, 12, 755–767, 1998.

Liu, Y., Weerts, A., Clark, M., Franssen, H. H., Kumar, S., Moradkhani, H., Seo, D., Schwanenberg, D., Smith, P., Van Dijk, A., et al.: Toward advancing data assimilation in operational hydrologic forecasting and water resources management: current status, challenges, and emerging opportunities, Hydrol. Earth Syst. Sci, 16, 3863–3887, 2012.

Maidment, D. R. et al.: Handbook of hydrology, vol. 1, McGraw-Hill New York, 1993.

Marchi, L., Borga, M., Preciso, E., and Gaume, E.: Characterisation of selected extreme flash floods in Europe and implications for flood risk management, Journal of Hydrology, 394, 118–133, 2010.

Masson, V., Champeaux, J.-L., Chauvin, F., Meriguet, C., and Lacaze, R.: A global database of land surface parameters at 1-km resolution in meteorological and climate models, Journal of climate, 16, 1261–1282, 2003.

McBride, J. L. and Ebert, E. E.: Verification of quantitative precipitation forecasts from operational numerical weather prediction models over Australia, Weather and Forecasting, 15, 103–121, 2000.

Nachtergaele, F., van Velthuizen, H., Verelst, L., Wiberg, D., Batjes, N., Dijkshoorn, K., van Engelen, V., Fischer, G., Jones, A., and Montanarela, L.: The harmonized world soil database. Version 1.2, in: Harmonized World Soil Database (version 1.2). FAO, Rome, Italy and IIASA, Laxenburg, Austria., 2012.

Nash, J. E. and Sutcliffe, J. V.: River flow forecasting through conceptual models part I—A discussion of principles, Journal of hydrology, 10, 282–290, 1970.

Noilhan, J. and Planton, S.: A simple parameterization of land surface processes for meteorological models, Monthly Weather Review, 117, 536–549, 1989.

Nuissier, O., Marsigli, C., Vincendon, B., Hally, A., Bouttier, F., Montani, A., and Paccagnella, T.: Evaluation of two convection-permitting ensemble systems in the HyMeX Special Observation Period (SOP1) framework, Quarterly Journal of the Royal Meteorological Society, 142, 404–418, 2016.

Payrastre, O., Lebouc, L., Ayral, P. A., Brunet, P., Delrieu, G., Douvinet, J., Dramais, G., Javelle, P., Johannet, A., Adamovic, M., et al.: The October 2015 flash-floods in south eastern France: first discharge estimations and comparison with other flash-floods documented in the framework of the Hymex project, in: EGU General Assembly Conference Abstracts, vol. 18, p. 13912, 2016.

Payrastre, O. et al.: Hydrological post event survey after the autumn 2014 floods in the Cévennes region in France: results and first hydrological analyses, in: 9th HyMeX workshop, 21-25 September 2015, Mykonos, Greece, 2015.

Pellarin, T., Delrieu, G., Saulnier, G.-M., Andrieu, H., Vignal, B., and Creutin, J.-D.: Hydrologic visibility of weather radar systems operating in mountainous regions: Case study for the Ardeche catchment (France), Journal of Hydrometeorology, 3, 539–555, 2002.

Piotte, O., Boura, C., Cazaubon, A., Chaléon, C., Chambon, D., Guillevic, G., Pasquet, F., Perherin, C., and Raimbault, E.: Collection, storage and management of high-water marks data: praxis and recommendations, in: E3S Web of Conferences, vol. 7, p. 16003, EDP Sciences, 2016.

Ricard, D., Ducrocq, V., and Auger, L.: A climatology of the mesoscale environment associated with heavily precipitating events over a northwestern Mediterranean area, Journal of applied meteorology and climatology, 51, 468–488, 2012.

Roux, H., Labat, D., Garambois, P.-A., Maubourguet, M.-M., Chorda, J., and Dartus, D.: A physically-based parsimonious hydrological model for flash floods in Mediterranean catchments, Natural Hazards & Earth System Sciences, 11, 2567–2582, 2011.

Rozalis, S., Morin, E., Yair, Y., and Price, C.: Flash flood prediction using an uncalibrated hydrological model and radar rainfall data in a Mediterranean watershed under changing hydrological conditions, Journal of hydrology, 394, 245–255, 2010.

Saint-Martin, C., Javelle, P., and Vinet, F.: DamaGIS: a multisource geodatabase for collection of flood-related damage data, Earth System Science Data Discussions, 2018, 1–18, https://doi.org/10.5194/essd-2018-28, https://www.earth-syst-sci-data-discuss.net/essd-2018-28/, 2018.

Savenije, H.: HESS Opinions" Topography driven conceptual modelling (FLEX-Topo)", Hydrology and Earth System Sciences, 14, 2681–2692, 2010.

Schaake, J. C., Hamill, T. M., Buizza, R., and Clark, M.: HEPEX: the hydrological ensemble prediction experiment, Bulletin of the American Meteorological Society, 88, 1541–1547, 2007.

SCS: SCS National Engineering Handbook Soil Conservation Service,, US Department of Agriculture, Washington DC., 1964.

Sharifi, A. and Kalin, L.: Effect of land use uncertainty on watershed modeling, in: World Environmental and Water Resources Congress 2010: Challenges of Change, pp. 4730–4739, 2010.

Silvestro, F. and Rebora, N.: Impact of precipitation forecast uncertainties and initial soil moisture conditions on a probabilistic flood forecasting chain, Journal of hydrology, 519, 1052–1067, 2014.

Tubiello, F. N., Biancalani, R., Salvatore, M., Rossi, S., and Conchedda, G.: A worldwide assessment of greenhouse gas emissions from drained organic soils, Sustainability, 8, 371, 2016.

Van Steenbergen, N. and Willems, P.: Rainfall uncertainty in flood forecasting: Belgian case study of Rivierbeek, Journal of Hydrologic Engineering, 19, 05014 013, 2014.

Vázquez, R., Feyen, L., Feyen, J., and Refsgaard, J.: Effect of grid size on effective parameters and model performance of the MIKE-SHE code, Hydrological processes, 16, 355–372, 2002.

Vincendon, B., Ducrocq, V., Nuissier, O., and Vié, B.: Perturbation of convection-permitting NWP forecasts for flash-flood ensemble forecasting, Natural Hazards and Earth System Sciences, 11, 1529–1544, 2011.

Vincendon, B., Édouard, S., Dewaele, H., Ducrocq, V., Lespinas, F., Delrieu, G., and Anquetin, S.: Modeling flash floods in southern France for road management purposes, Journal of Hydrology, 541, 190–205, 2016.

Vivoni, E. R., Entekhabi, D., and Hoffman, R. N.: Error propagation of radar rainfall nowcasting fields through a fully distributed flood forecasting model, Journal of Applied Meteorology and Climatology, 46, 932–940, 2007.

Yen, H., Sharifi, A., Kalin, L., Mirhosseini, G., and Arnold, J. G.: Assessment of model predictions and parameter transferability by alternative land use data on watershed modeling, Journal of hydrology, 527, 458–470, 2015.

Zalachori, I., Ramos, M.-H., Garçon, R., Mathevet, T., and Gailhard, J.: Statistical processing of forecasts for hydrological ensemble prediction: a comparative study of different bias correction strategies, Advances in Science and Research, 8, 135–141, 2012.

Zappa, M., Jaun, S., Germann, U., Walser, A., and Fundel, F.: Superposition of three sources of uncertainties in operational flood forecasting chains, Atmospheric Research, 100, 246–262, 2011.

FIGURES

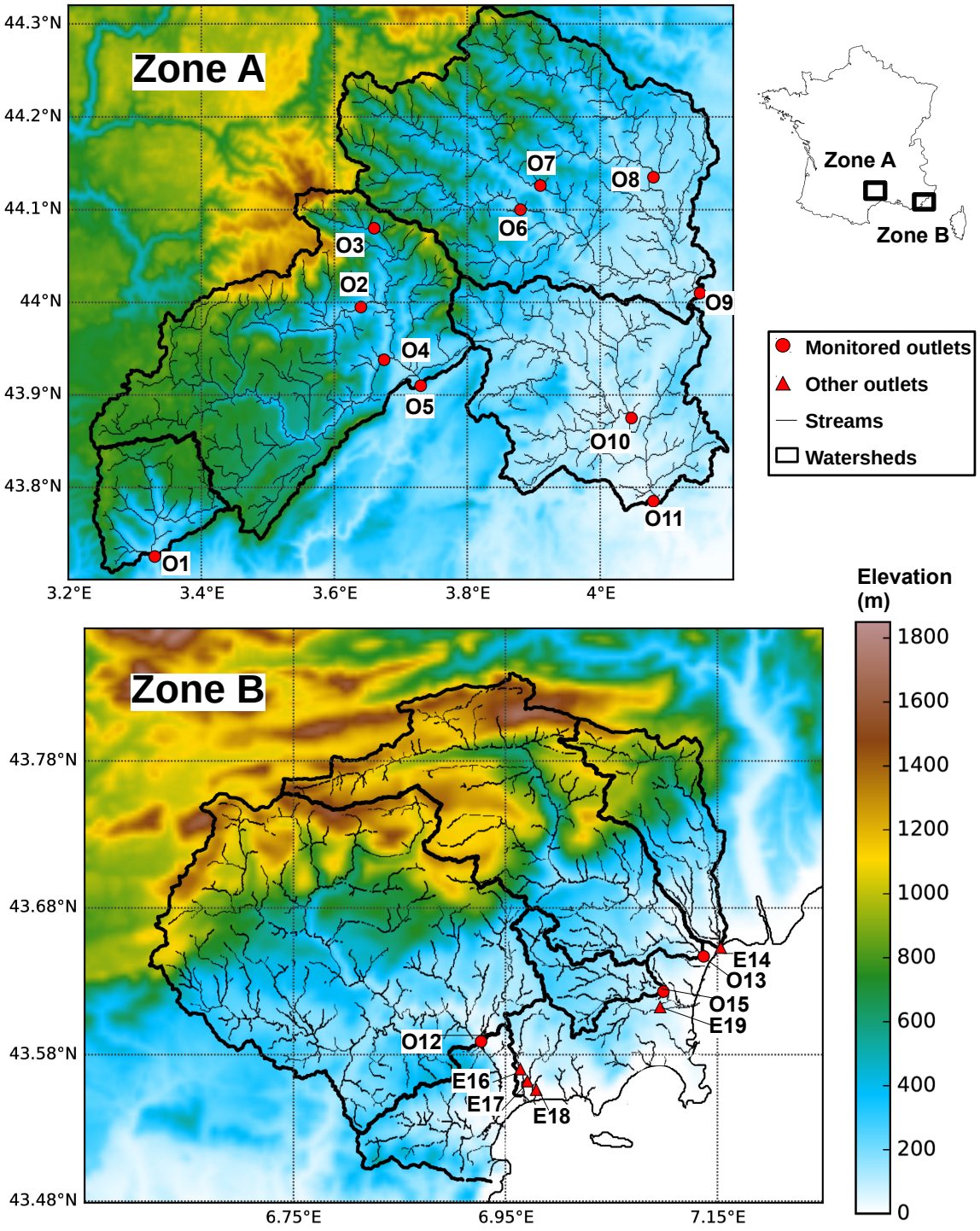

Figure 1. Location of the study areas, zones A and B, and boundaries of the main watersheds of both areas. The red markers correspond to the studied outlets. The circular outlets are monitored. Coordinates are in WGS84. The elevation was obtained from the SRTM dataset.

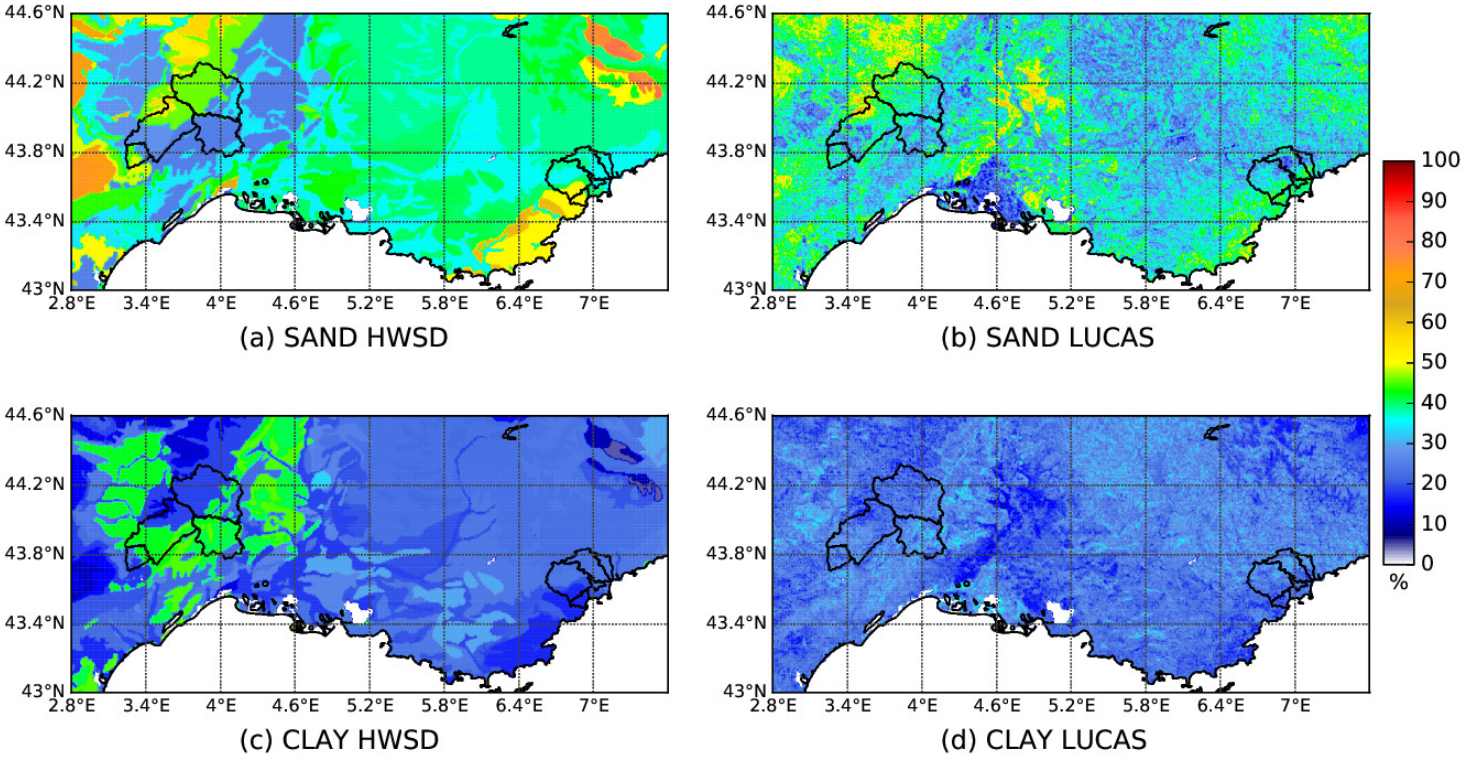

Figure 2. Soil texture over southeastern France: fraction of sand from (a) HWSD and (b) LUCAS and fraction of clay from (c) HWSD and (d) LUCAS. The catchments of zones A and B are delineated in black.

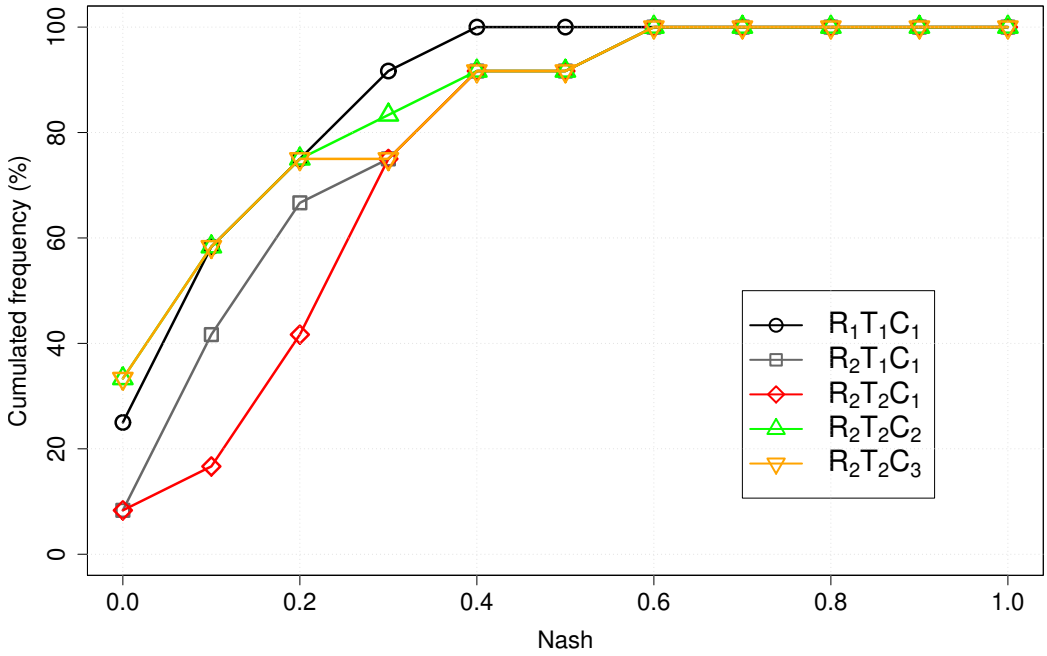

Figure 3. Cumulated frequency of the Nash values for each watershed in zone A for each experiment.

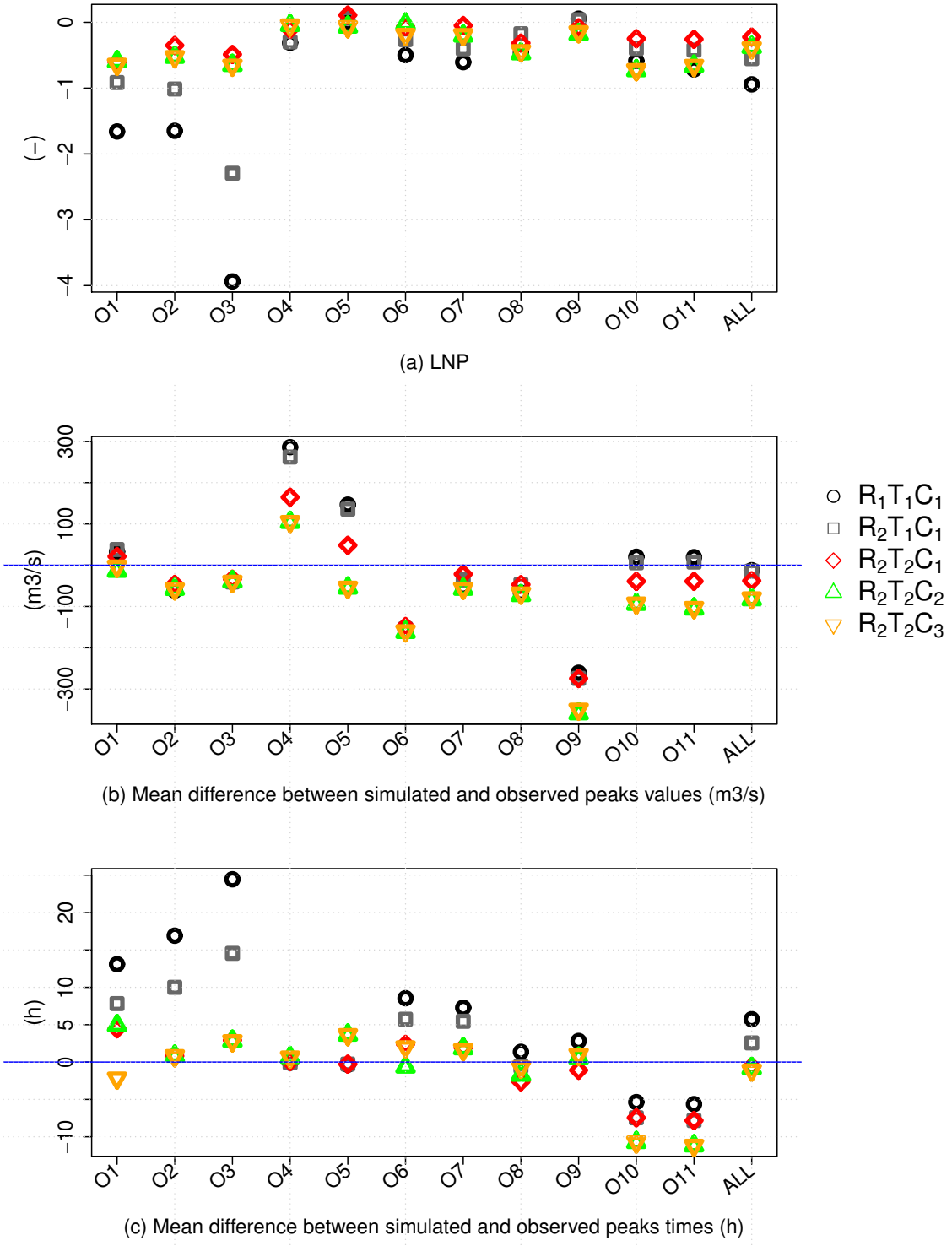

Figure 4. Scores for each watershed in zone A and all the outlets, for the $R_1T_1C_1$–$R_2T_2C_3$ experiments.

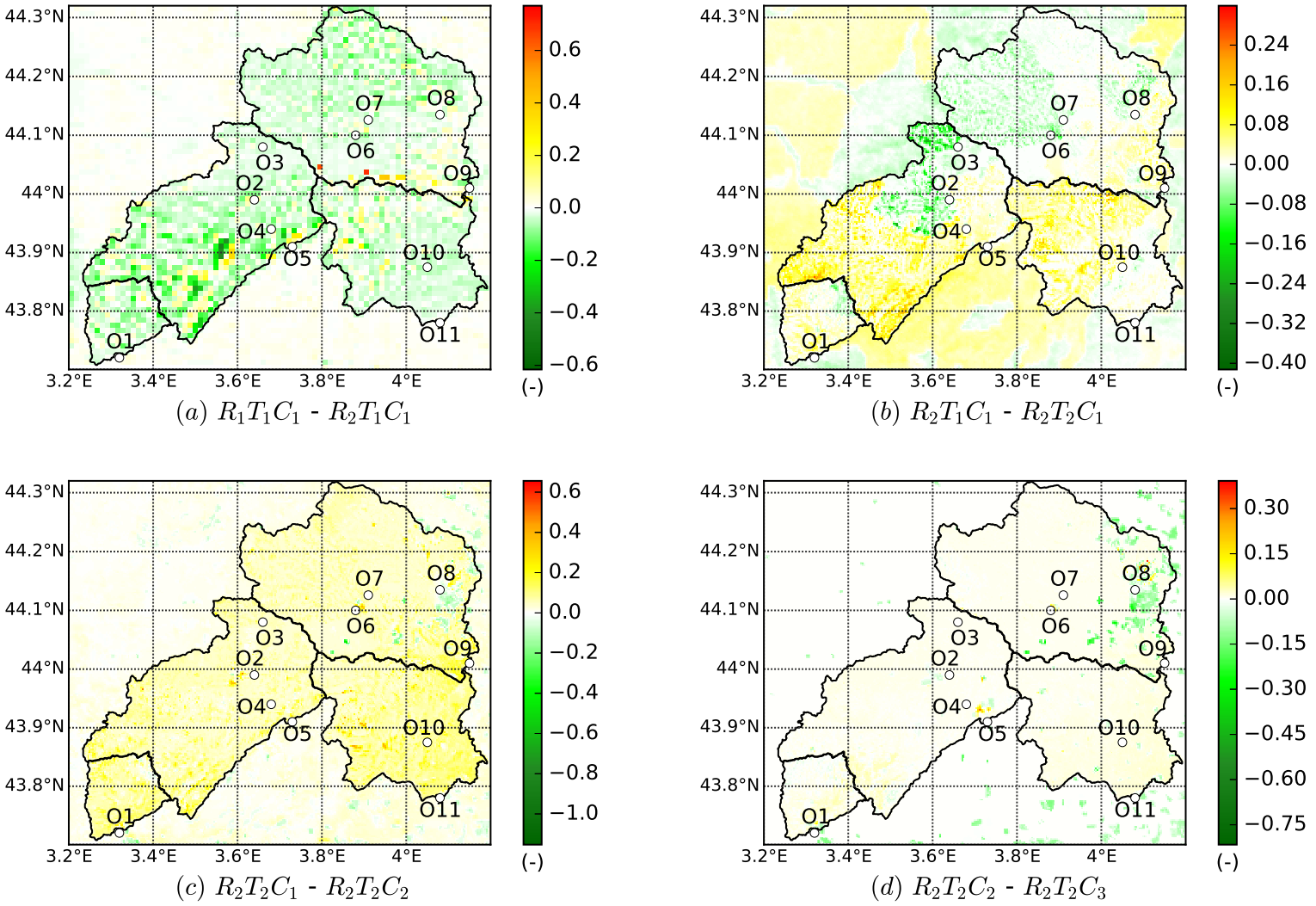

Figure 5. Mean differences in the ratios of the runoff amounts to the rainfall amounts (without units) (a) between $R_1T_1C_1$ and $R_2T_1C_1$, (b) between $R_2T_1C_1$ and $R_2T_2C_1$, (c) between $R_2T_2C_1$ and $R_2T_2C_2$ and (d) between $R_2T_2C_2$ and $R_2T_2C_3$. Note that the range of the colour scale is not the same for the various panels; however, in red/yellow, the differences are always positive and, in green, they are always negative.

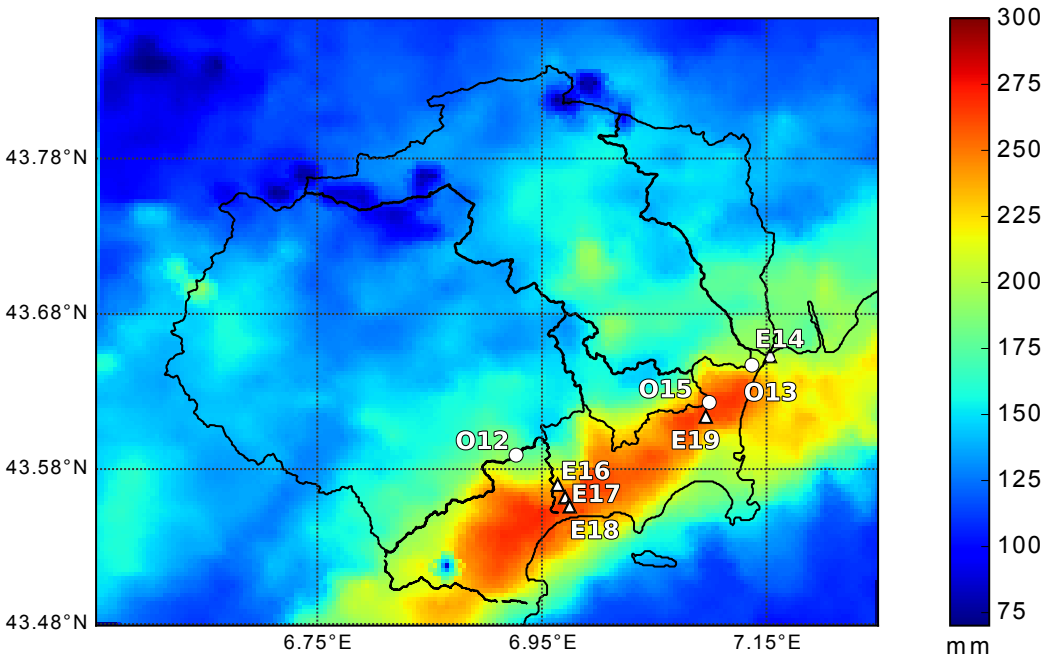

Figure 6. Cumulated rainfall over zone B during the October 2015 event for the Pégomas (O12), Villeneuve-Loubet (O13), Biot (O15) and Cannes (E18) locations.

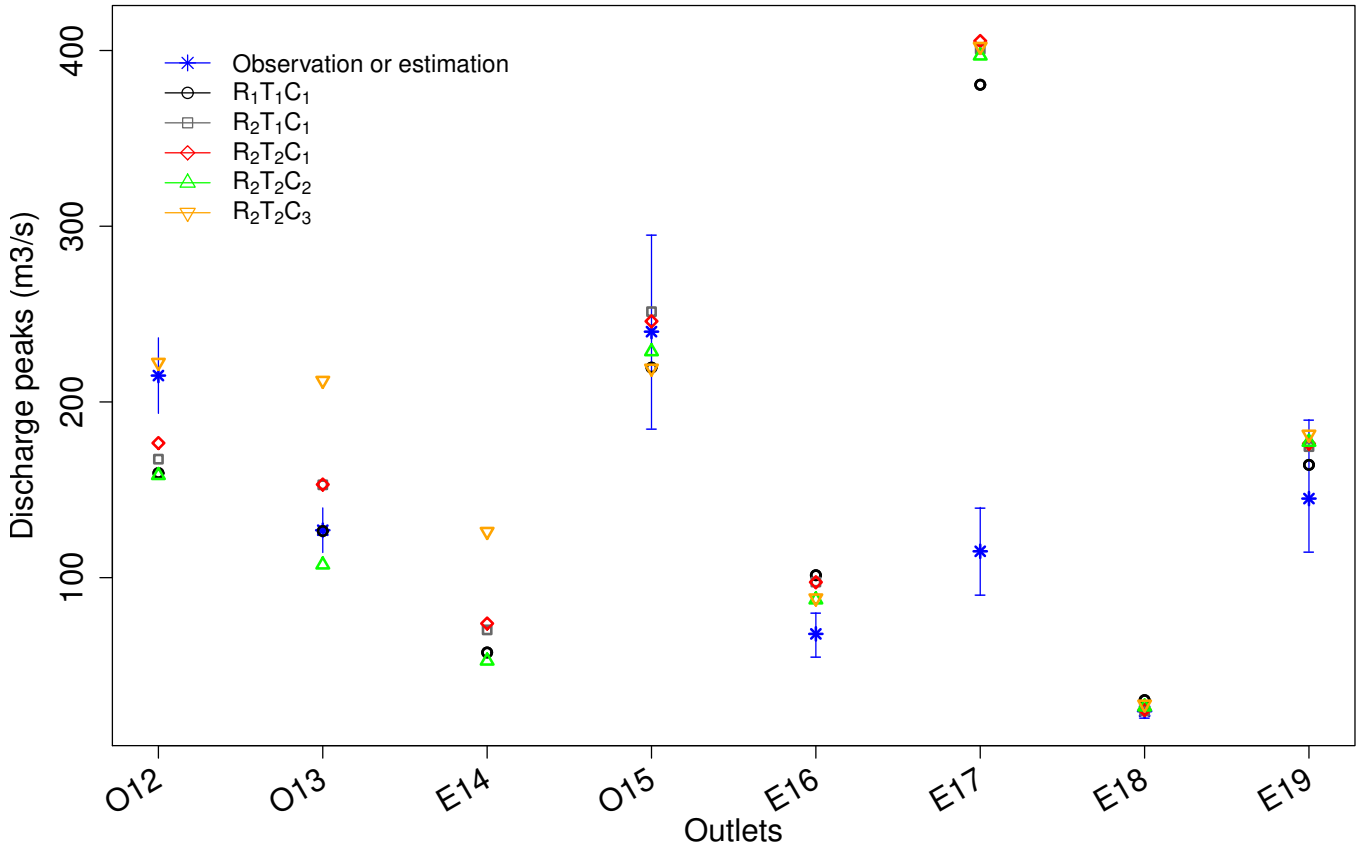

Figure 7. Discharge peaks ($m^3\ s^{-1}$) observed or estimated in blue and simulated by the $R_1T_1C_1$–$R_2T_2C_3$ experiments for each catchment for the October 2015 event. The error margins (blue segments) in the observed values (O#) are approximately 10%, and the error margins for the others (E#) were estimated using post-event surveys. Only the damage was registered for E14 during this event; therefore, no estimate is available. For E18, the discharge values ranged between 20 $m^3\ s^{-1}$ and 28 $m^3\ s^{-1}$.

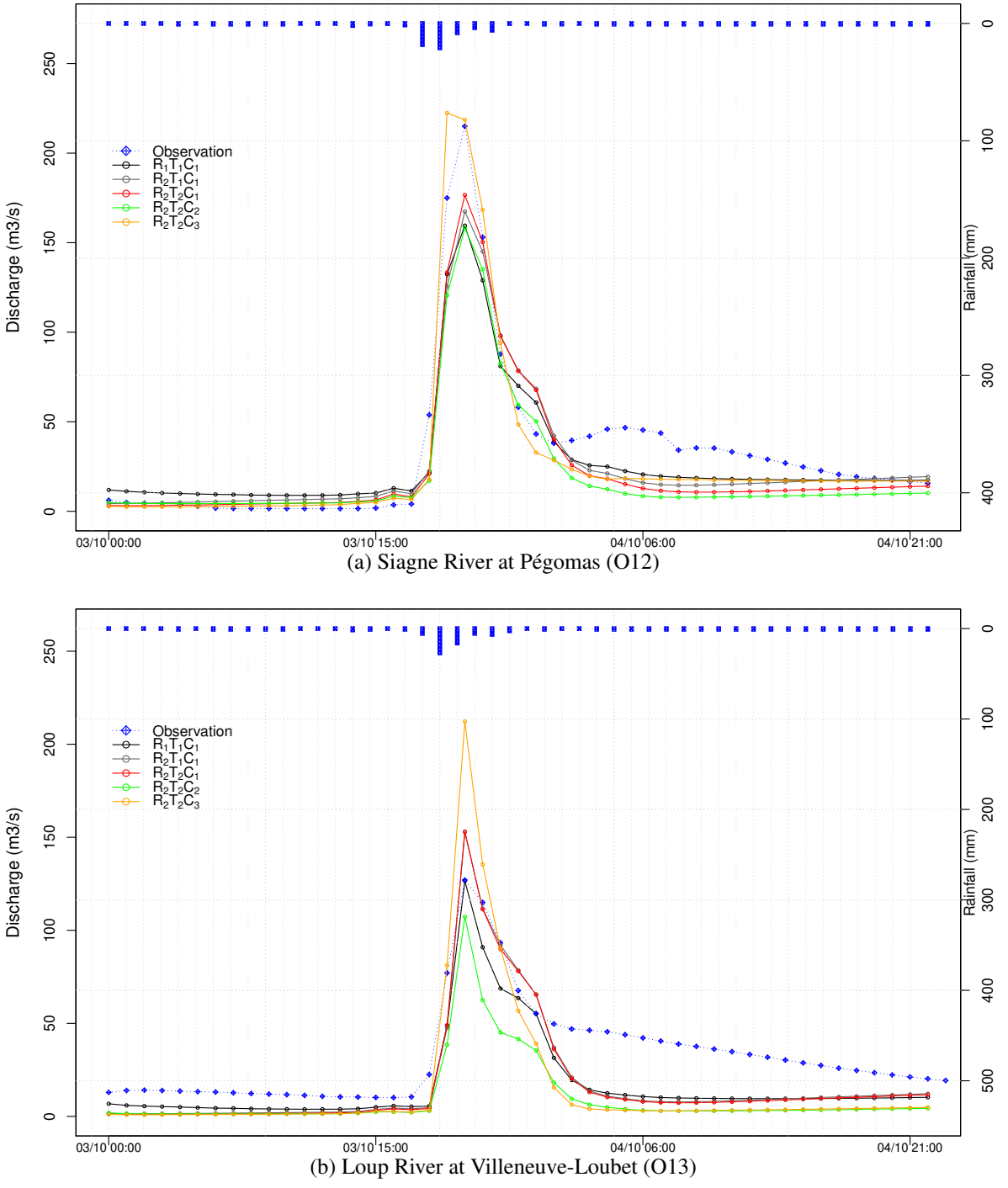

Figure 8. Discharge time series observed (blue curve) and simulated by ISBA-TOP in the five experiments $R_1T_1C_1$–$R_2T_2C_3$ for 03 October 2015 for (a) the Siagne River at Pégomas and (b) the Loup River at Villeneuve-Loubet. The reverse histogram represents the hourly rainfall averaged over the catchment.

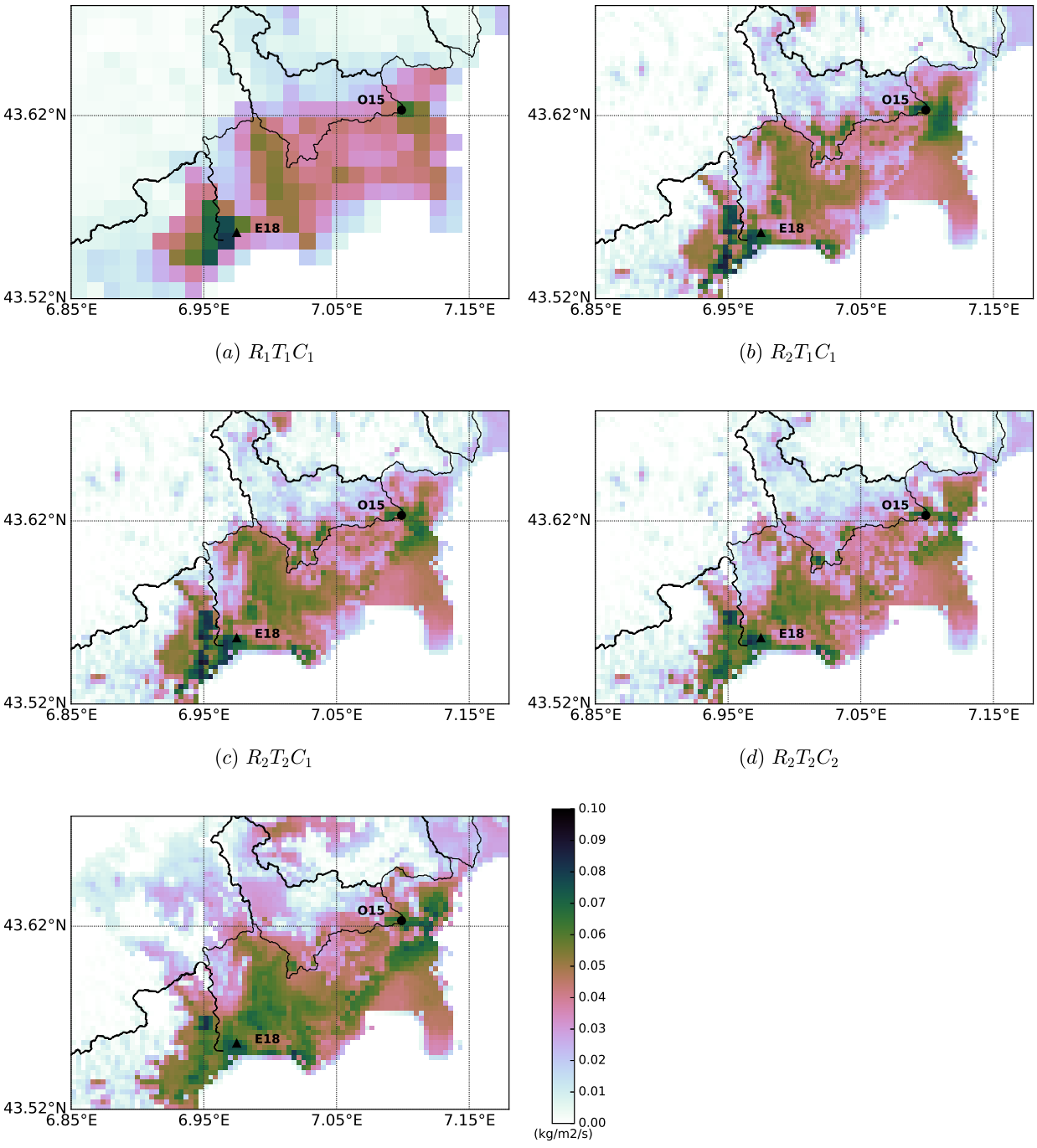

(a) $R_1T_1C_1$ (b) $R_2T_1C_1$

(c) $R_2T_2C_1$ (d) $R_2T_2C_2$

(e) $R_2T_2C_3$

Figure 9. Cumulated runoff for each experiment for the October 2015 event.

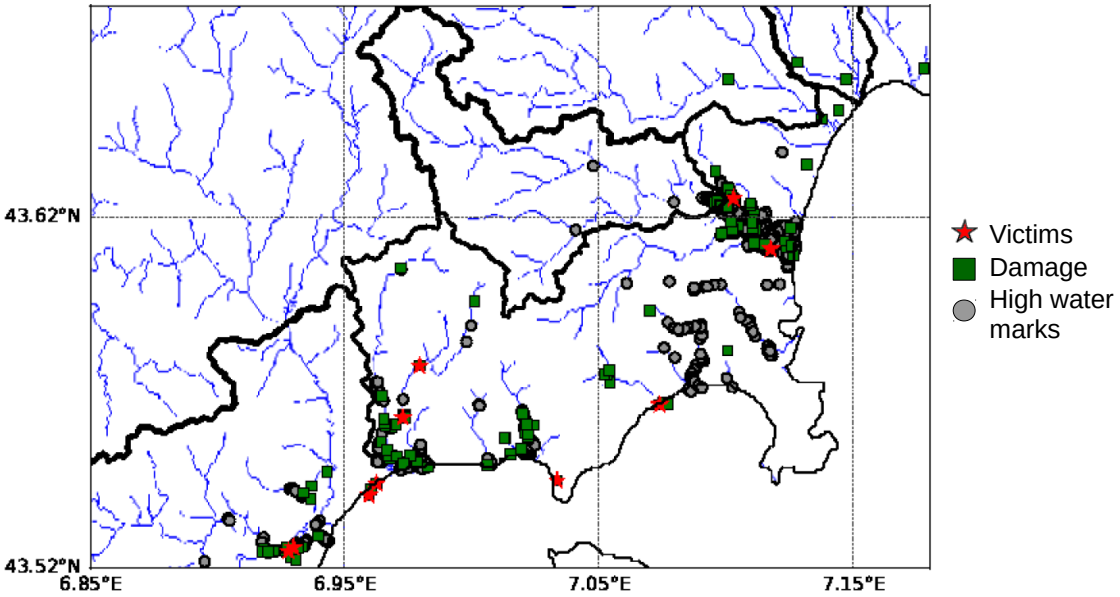

Figure 10. Impact map with the stream network. Locations of the victims are shown in red, damage is shown in green and high-water marks are shown in grey. Fatalities and damage locations were provided by the multisource geodatabase DamaGIS (Saint-Martin et al., 2018).

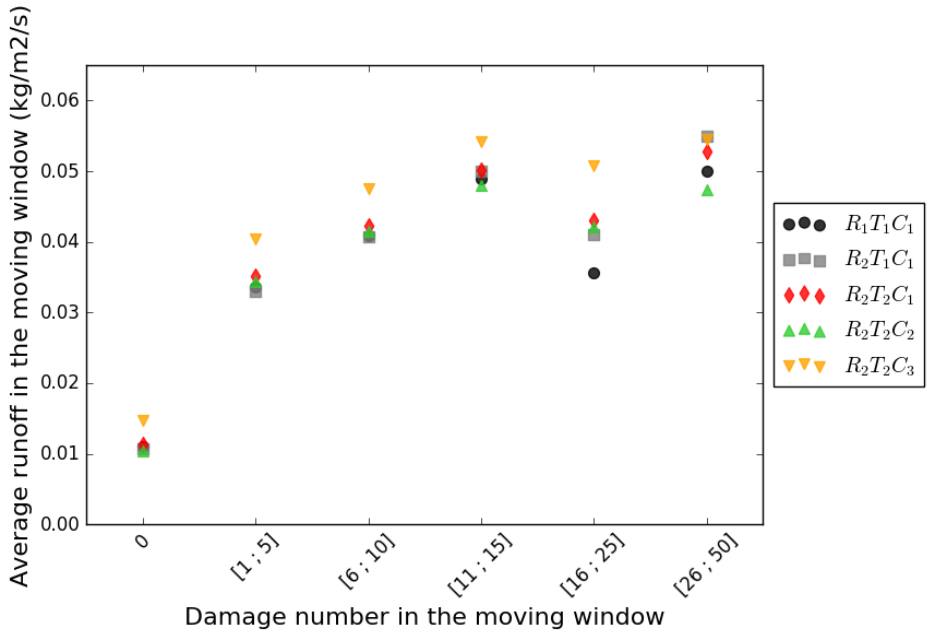

Figure 11. Average runoff in function of the number of damages encountered in the 1-km circular neighbourhood over all the domain of Figure 9.

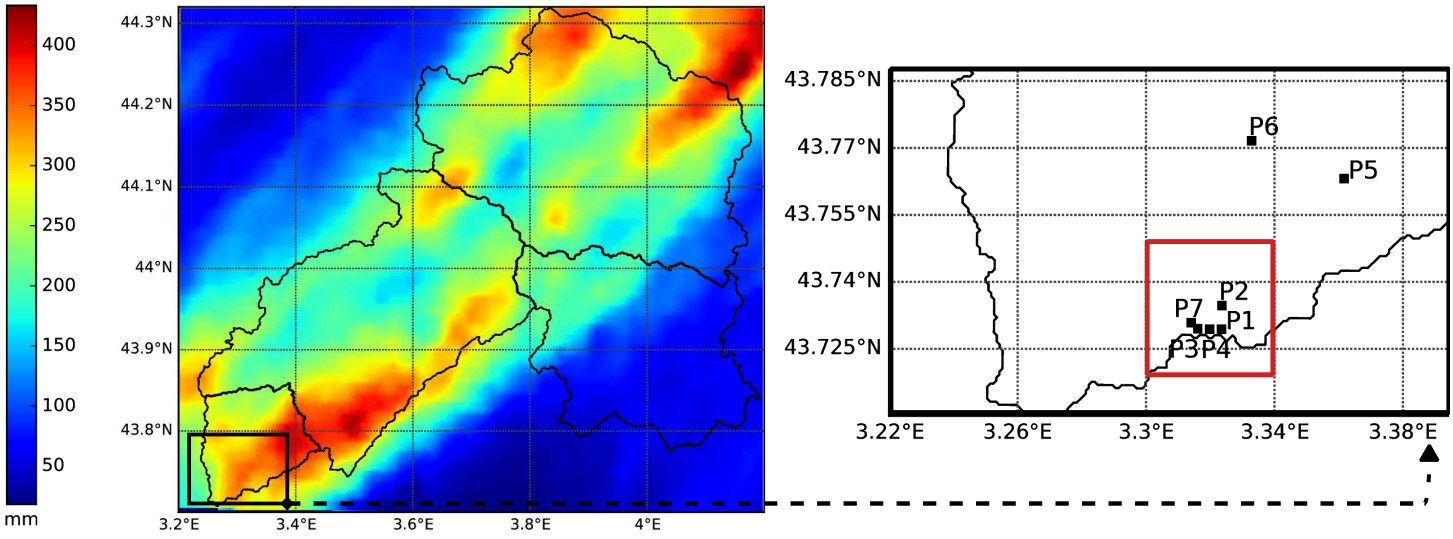

Figure 12. Cumulated rainfall during the 12 September 2015 event and the location of points P1–P7 (black squares) within the Lergue catchment in zone A.

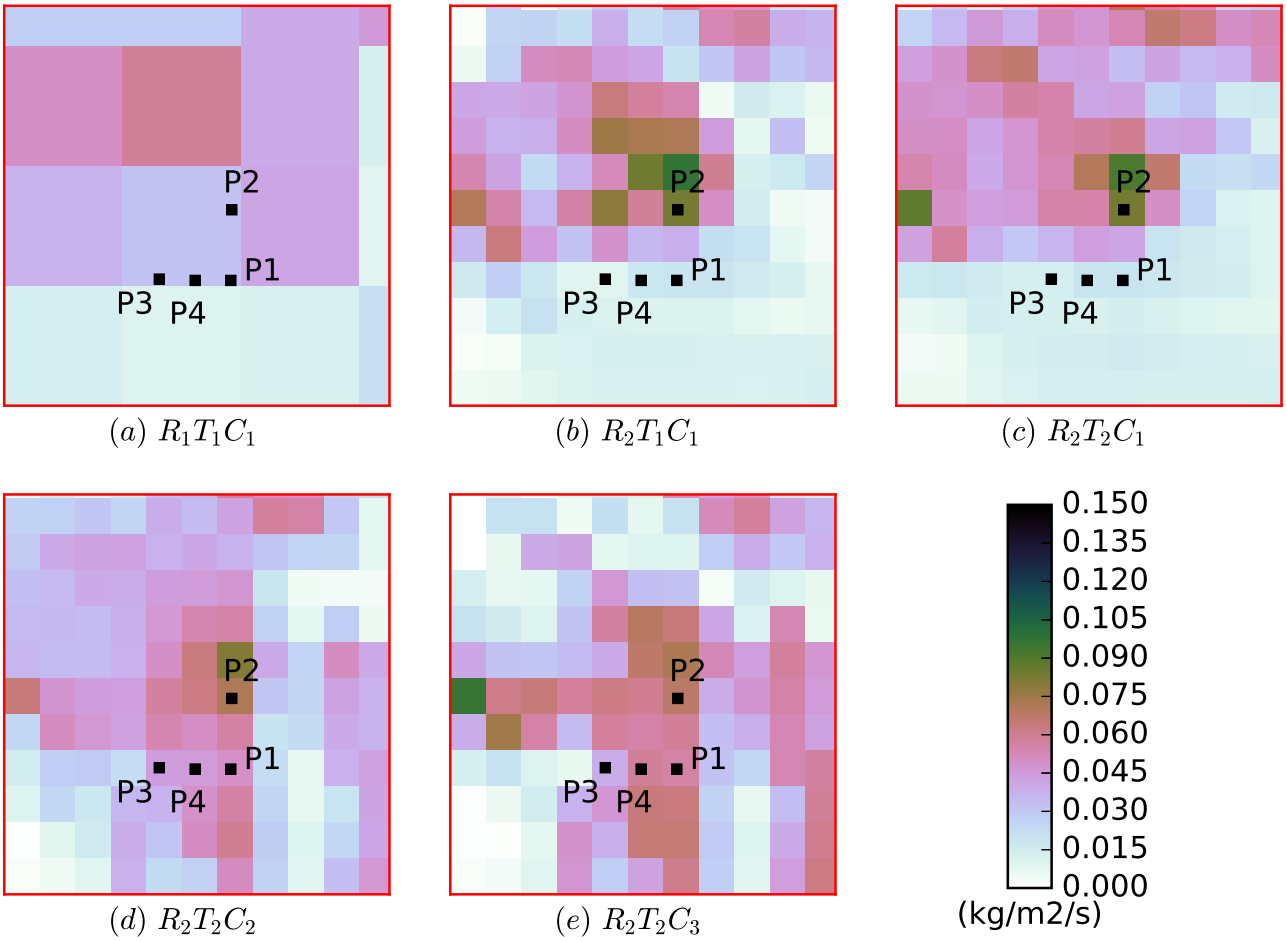

Figure 13. Cumulated runoff during the September 2015 event for $R_2T_1C_1$–$R_2T_2C_3$ and the locations of points P1–P4.

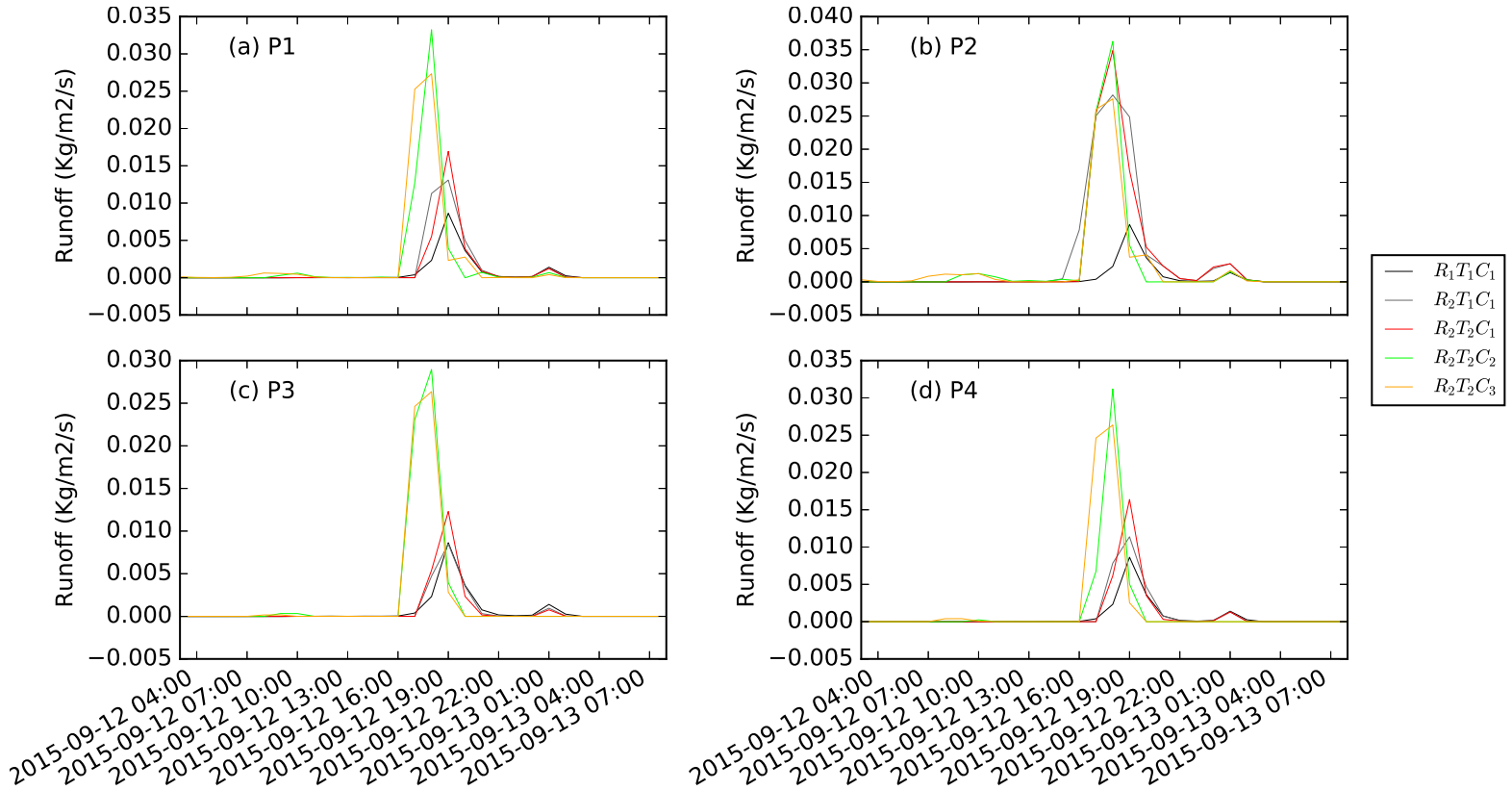

Figure 14. Runoff time series between 03 UTC on 12 September 2015 and 08 UTC on 13 September 2015 at (a) P1, (b) P2, (c) P3 and (d) P4.

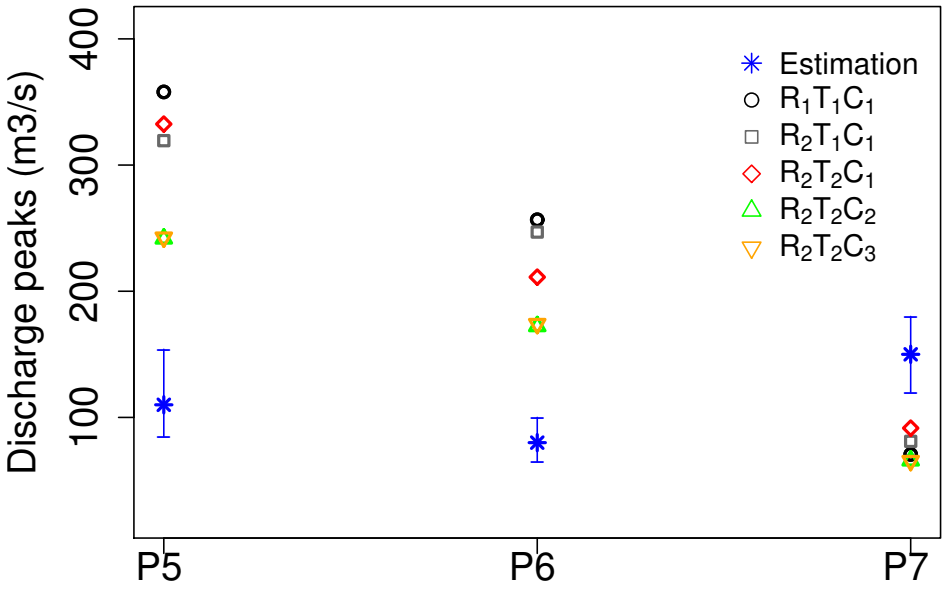

Figure 15. Estimated or simulated peak flows ($m^3\ s^{-1}$) during the September 2015 event. The error margins (blue segments) of the peak values were estimated using post-event surveys.

TABLES

Table 1. Characteristics of the main studied catchments and outlets. Their locations are given in Figure 1 from west to east within each catchment. The basin characteristic times, presented in Appendix A, are reported here.

	River	Outlets	Name	Area (km^2)	tc (h)	tb (h)
Zone A	Lergue	**Lodève**	O1	181	3.2	1.9
	Hérault	Vigan [La Terrisse]	O2			
		Valleraugue	O3			
		St Laurent le Minier	O4			
		Laroque	O5	918	10.2	6.1
	Gardon	St Jean du Gard	O6			
		Mialet	O7			
		Alès	O8			
		Ners	O9	1092	8.8	5.3
	Vidourle	Vic-le-Fesq	O10			
		Sommières	O11	621	8.8	5.3
Zone B	Siagne	**Pégomas**	O12	515	11.3	6.8
	Loup	**Villeneuve-Loubet**	O13	278	12	7.2
	Cagne	**Cagnes-sur-mer**	E14	109	7.6	4.5
	Brague	**Biot**	O15	41	6	3.6
	Eastern coastal zone	Ranguin	E16			
		Mougins	E17			
		Cannes	E18			
		Biot [Gorges]	E19			

Table 2. Characteristics of the flash-flood events.

	Starting day of the event	Duration (h)	Maximum cumulative rainfall observed (mm)
Zone A	17/09/2014	72	415.5
	11/10/2014	73	105.9
	28/11/2014	49	228.9
	12/09/2015	73	390
	28/10/2015	73	179.2
	03/11/2015	73	157.5
	05/04/2016	49	111
	10/05/2016	73	86.5
	14/10/2016	49	69.6
	21/11/2016	73	287.5
	24/11/2016	73	143.1
Zone B	03/10/2015	72	277.1

Table 3. Mean soil texture fractions per watershed from the HWSD and LUCAS topsoils and fraction of the land use types from ECO-CLIMAP II and ECO-SG.

		ZONE A				ZONE B			
		Lergue O1	Hérault O5	Gardon O9	Vidourle O11	Siagne O12	Loup O13	Cagne E14	Brague O15
Clay	HWSD	30.6	32.2	23.7	38.2	21.5	23.5	23.8	23.9
%	LUCAS	25.3	24.2	23.6	26.7	24.9	26.3	26.3	23.8
Sand	HWSD	38.2	35.6	40.4	26.9	40.7	37.6	36.6	36.1
%	LUCAS	33.9	36.8	38.5	32.3	33.5	31.3	31.6	39.1
Water	ECOCLIMAP	-	-	-	-	-	-	0.1	-
%	ECO-SG	-	-	0.1	-	0.5	-	-	-
Forests	ECOCLIMAP	50.5	48	55.6	40	48.1	37.6	23.3	32.1
%	ECO-SG	40.9	53.1	74.4	57.2	42.5	29.8	14.8	31.3
Shrubs/ herbaceous/ grassland %	Eoclimap	29.7	33.4	28	31.8	27.3	31	23	23.4
	ECO-SG	31.4	25.3	6	7.5	22.7	35.5	35.7	4.6
Crops	ECOCLIMAP	10.1	9.6	6.7	10.3	7.5	12.5	12.6	4.3
%	ECO-SG	25.8	20.1	13.1	32.7	18.5	19.1	16.9	10.5
Urban/bare soil	ECOCLIMAP	9.7	9	9.7	17.9	17.1	18.9	41	40.2
%	ECO-SG	1.9	1.5	6.4	2.6	15.8	15.6	32.6	53.6

Table 4. Experimental parameters.

Simulations	ISBA-TOP RESOLUTION (R)		TEXTURE (T)		LAND COVER (C)		
NAMES	1000 m	300 m	HWSD	LUCAS	ECOCLIMAP	ECO-SG	ECO-SG Town to Rock
$R_1T_1C_1$	X		X		X		
$R_2T_1C_1$		X	X		X		
$R_2T_2C_1$		X		X	X		
$R_2T_2C_2$		X		X		X	
$R_2T_2C_3$		X		X			X

Table 5. High-water marks for points P1–P4 for the September 2015 event.

Point	Water level (m)
P1	1.02
P2	0.94
P3	0.75
P4	1.45